Research Square

Preprints are preliminary reports that have not undergone peer review.
They should not be considered conclusive, used to inform clinical practice,
or referenced by the media as validated information.

Projecting maize yield in the North China Plain under climate extremes: A hybrid crop model-machine learning approach

Haonan Tan

tanhn223@163.com

Hebei Normal University https://orcid.org/0009-0002-8327-122X

Dengpan Xiao

Hebei Normal University https://orcid.org/0000-0001-6900-1237

Huizi Bai

Hebei Academy of Sciences

Yang Lu

Hebei Normal University

Lihua Lv

Hebei Academy of Agriculture and Forestry Sciences

Peipei Pan

Hebei Normal University

Dandan Ren

Linyi University

Man Zhang

Hebei Normal University

Xiaomeng Yin

Hebei Normal University

Yan Wang

Hebei Normal University

Ying Li

CMA Henan Agrometerological Support and Applied Techque key laboratory

Chen Wang

Hebei Normal University

Maoyuan Sun

Hebei Normal University

Research Article

Keywords: Extreme climate, APSIM Model, Machine learning, Maize, CO2 fertilization

Posted Date: August 14th, 2026

DOI: https://doi.org/10.21203/rs.3.rs-9895808/v1

License: This work is licensed under a Creative Commons Attribution 4.0 International License.
Read Full License

Projecting maize yield in the North China Plain under climate extremes: A hybrid crop model-machine learning approach

Abstract

Process-based crop models are effective tools for assessing the impact of climate change on crop yields, but they have limitations in accurately describing the effects of extreme climate events on yields. We constructed a hybrid simulation framework that integrates a process-based model (APSIM) with machine learning (ML) models, i.e., random forest (RF) and light gradient boosting machine (LGBM). We applied two feature selection techniques, i.e., stepwise regression (SR) and genetic algorithm (GA), to identify the most informative extreme climate indicators (ECIs) for specific growth stages. These selected ECIs, along with the outputs of the APSIM, were then incorporated into the RF and LGBM to evaluate the impacts of extreme climate on maize yields in the North China Plain. Overall, the hybrid model significantly improved the accuracy of yield predictions, and APSIM+RF+GA was the best model for estimating yields, explaining 94% and 93% of the observed yield variations for spring and summer maize, respectively. Compared to APSIM alone, the hybrid model improved simulation accuracy by 30% and 31% for spring and summer maize, respectively. Overall, the APSIM+RF+GA projected significantly greater yield losses than the standalone APSIM, highlighting its superior ability to capture the severe impacts of extreme climate events. For future simulation under SSP585_2080s scenario, the hybrid model predicted yield losses of 43.6% for spring maize and 26.8% for summer maize without the carbon dioxide (CO_2) fertilization effect. With the CO_2 considered, the hybrid model still predicted yield losses of 25.0% for spring maize and 24.6% for summer maize. Although elevated future CO_2 concentrations exerted a significant positive effect on maize yield, this benefit was far from sufficient to offset the negative impacts of climate change. Overall, the hybrid model developed in this study addresses the limitations inherent in standalone process-based models and demonstrates stronger suitability for forecasting future crop yields.

Keywords: Extreme climate; APSIM Model; Machine learning; Maize; CO_2 fertilization

1. Introduction

The Sixth Assessment Report of the United Nations Intergovernmental Panel on Climate Change (IPCC6) shows that the global surface temperature in 2011–2020 increased by 1.1℃ compared with 1850–1900 (IPCC, 2022). With global climate warming, the frequency and intensity of extreme weather events have increased significantly in many regions and are projected to intensify further in the future (Hu et al., 2024; Sutanto et al., 2025). In China, the temperature rise rate has obviously exceeded the global average during the same period (Jiang et al., 2025), and the frequency and intensity of extreme climate events have significantly increased, which exerted a negative impact on agricultural production, and also brought unfavorable factors to food supply security (Xiao et al., 2022). Therefore, it is necessary to accurately estimate the yield losses caused by current and future extreme climate events in order to assess the sustainability of crop production.

Maize, one of the world's three major food crops, plays a vital role in safeguarding global food security. As the second-largest maize producer, China accounts for 21% of the global cultivation area and 23% of the global maize supply (NBS, 2022). Within China, the North China Plain (NCP) maize belt constitutes the primary production region, contributing 30% of the national total output (Liu et al., 2021). However, compared with other major staple crops, maize exhibits the greatest sensitivity to extreme climate events (Tang et al., 2025). While previous studies have predominantly focused on the impacts of mean climate change on crop production, recent research has increasingly shifted toward the effects of extreme climate events (Xiao et al., 2022). This shift is particularly relevant for the NCP, where climate warming has led to a sharp increase in the frequency of droughts and extreme rainfall events (Ji et al., 2025).

Initially, various statistical regression methods are employed to investigate the relationship between climate change and crop yields. The primary advantage of these statistical models lies in their simplicity and ease of application. However, traditional statistical regression models typically presuppose a linear relationship among agro-ecosystem parameters, environmental variables, and management factors. In contrast, the relationship between crop yield and factors such as climatic variables is often complex and nonlinear (Dehnavi et al., 2020). As advanced statistical models, machine learning algorithms are increasingly recognized as a cutting-edge approach for investigating climate-yield relationships, primarily due to their capacity to capture these complex

nonlinear associations between predictors and responses (Jeong et al., 2016; Erfanian et al., 2022). Nevertheless, a key limitation persists: statistical models, including machine learning, primarily establish correlations between climate and yield while often overlooking the underlying physiological metabolism and ecological processes of the crops themselves (Roberts et al., 2017; Patil et al., 2024). In contrast to statistical models, crop simulation models have been widely employed to reveal the impacts of historical and future extreme climate events on crop yields, as they are designed to simulate physiological and ecological processes (Zeng et al., 2026). However, most crop models simplify the mechanisms by which extreme climate affects crop growth, development, and yield formation, leading to inherent uncertainties in their simulation results (Feng et al., 2019).

Given the complementary strengths and limitations of process-based crop models and statistical regression methods, a growing body of research has sought to integrate them, leveraging both mechanistic understanding and data-driven predictive power (Feng et al., 2020). One line of inquiry has focused on enhancing yield component prediction. For instance, Jahangirlou et al. (2023) coupled the APSIM-maize model with a three-parameter logistic regression to accurately predict maize grain starch, oil, and protein contents. Another key application has been improving yield prediction under extreme climate conditions. Sajid et al. (2022) demonstrated that integrating APSIM-simulated crop growth process data with soil, meteorological, and management variables into a machine learning framework significantly improved county-scale yield prediction accuracy across the US Maize Belt. However, their analysis focused primarily on water-related extreme climate indicators (ECIs) such as drought stress and groundwater level, without systematically considering other critical ECIs like high temperature and heavy precipitation. Furthermore, they considered only the frequency of ECIs, overlooking the well-established finding that maize sensitivity to extreme events varies markedly across growth stages, and that the intensity and duration of such events during key phenological phases profoundly influence yield formation. Addressing this temporal dimension, Shahhosseini et al. (2021) incorporated APSIM outputs and multiple agro-climatic indicators disaggregated by growth stage into a deep learning algorithm, successfully enhancing yield prediction accuracy at key phenological phases. Despite this advance, the inclusion of a large number of predictor variables in machine learning algorithms can lead to

increased computational costs and model overfitting—a challenge that becomes particularly acute in large-scale, county-level predictions (Klompenburg et al., 2020). This underscores the necessity of selecting the most informative variable subsets to mitigate the 'curse of dimensionality', accelerate model training, and improve model interpretability (Wang et al., 2018; Patil et al., 2024).

In this study, we developed a series of hybrid models by integrating the APSIM model with machine learning algorithms to assess the impacts of extreme climates on maize yield. Based on the frequency, intensity, and duration of extreme climate events frequently encountered by spring and summer maize in the NCP across three key growth stages, we designed three categories of ECIs, comprising a total of 22 extreme climate predictors. Through feature selection, we identified the most informative subset of these predictors for model input. The main objectives of this study are: (1) to systematically identify the key climatic factors affecting maize production in the NCP, with an emphasis on extreme climate indices; (2) to construct a hybrid simulation framework that couples a mechanistic crop model with machine learning, enabling a more comprehensive characterization of extreme climate impacts on crop growth processes; and (3) to apply this established framework to simulate and analyze maize yield under future climate scenarios incorporating extreme climate events, thereby providing a scientific basis for formulating regional agricultural adaptation strategies.

2. Material and methods

2.1 Study area

The NCP, located in eastern China, encompasses the provinces of Beijing, Tianjin, Hebei, Shandong, Shanxi, and Henan. Characterized by a warm temperate monsoon climate, the region experiences distinct seasonal changes and abundant solar and thermal resources. The annual precipitation varies between 500 and 1000 mm, with over 70% of rainfall concentrated from July to September. The dominant soil type is alluvial soil, formed by river sedimentation over geological periods. These favorable conditions make the NCP a major maize-producing area in China. This study focuses on both spring and summer maize growing areas within the NCP, utilizing data from 51 agricultural meteorological stations distributed across the region (Fig. 1). Spring maize is primarily cultivated in the western and northern parts of the NCP, typically sown from late April to early May and harvested in late September. In contrast, summer maize is sown in early June and

harvested in early October. Detailed information on crop management and climatic conditions for the 51 stations is provided in Table S1.

Insert Fig. 1 here.

2.2 Crop, climate and soil data

Daily historical meteorological data, including maximum temperature (Tmax), minimum temperature (Tmin), precipitation (Prec), wind speed, and sunshine duration, were obtained from the China Meteorological Administration (CMA). Corresponding crop data (e.g., variety, phenology, yield and management practices) were also provided by the CMA. Soil profile parameters, including bulk density, soil organic matter, total nitrogen, and pH, were extracted from the Harmonized World Soil Database (HWSD) Version 2.0.

Future climate projections were based on 27 global climate models (GCMs) from the Coupled Model Intercomparison Project Phase 6 (CMIP6) (Table S2). The raw GCM outputs, characterized by coarse spatial and temporal resolutions, are unsuitable for direct application in site-specific crop models. Therefore, we employed the statistical downscaling method developed by Liu and Zuo (2012) to convert the original monthly grid data into daily-scale meteorological series for each of the 51 stations. Two future scenarios were considered: SSP245, which integrates SSP2 with RCP4.5, and SSP585, which integrates SSP5 with RCP8.5.

2.3 APSIM model

APSIM (Agricultural Production Systems Simulator) is a biophysical model designed to simulate crop growth and development processes at the field scale (Holzworth et al., 2014). This model is capable of simulating outputs such as biomass and grain yield of various crops under the influences of climatic conditions, soil properties, and agricultural management practices. However, APSIM simplifies certain physiological and ecological processes during simulation and does not fully incorporate the response mechanisms of extreme climate events on crop yield. This is certain limitations in its yield simulation accuracy under extreme climatic conditions. In this study, the APSIM-maize version 7.9 was adopted to simulate the phenology, biomass, and yield of spring maize and summer maize at 51 stations in the NCP.

For the calibration period (1981–2009), we selected crop data from years with complete observational records, including yield and field management information, to calibrate cultivar-

related parameters. Subsequently, the APSIM-maize model was driven to simulate yield and phenology of maize across all stations in the NCP, strictly following experimental records for cultivar information, sowing date, planting density, irrigation, and fertilization. Finally, the simulated yield and phenology were directly compared with the corresponding observed data.

To assess the impacts of climate change, this study considers three 30-year periods: the historical baseline period (1981–2010) and two future periods with two climate scenarios (SSP245 and SSP585), namely 2031–2060 (2040s) and 2071–2100 (2080s). Model simulations were configured as follows. Cultivar parameters were set based on the prevalent cultivars at each station during 2006–2009, and sowing dates were determined using station-specific averages over the 1981–2009 period. Nitrogen fertilizer was applied at a rate of 200 kg ha^{-1} at both sowing and the big trumpet stage. Irrigation was managed using the automatic irrigation module embedded in APSIM. The atmospheric CO_2 concentration ($[CO_2]$) for the baseline period was set to 380 ppm. For the two future periods, annual $[CO_2]$ under the SSP245 and SSP585 scenarios were calculated using empirical equations (1) and (2), respectively (O'Neill et al., 2016).

$$[CO_2]_{SSP245}=62.044+\frac{34.002-3.8702y}{0.24423-1.1542y^{2.4901}}+0.028057x(y-1900)^2+0.00026827\times (y-1960)^3-9.2751\times10^{-7}\times(y-1910)^4-2.2448\times(y-2030) \quad (1)$$

$$[CO_2]_{SSP585}=757.44+\frac{84.938-1.517y}{2.2011-3.8289y^{0.45242}}+2.4712\times10^{-4}\times(y+15)^2+1.9299\times10^{-5}\times (y-1937)^3+5.11137\times10^{-7}\times(y-1910)^4 \quad (2)$$

Where y denotes relate year.

2.4 Extreme climate indices (ECIs)

For drought assessment, we selected two drought indices: the Standardized Precipitation Index (SPI) and the Standardized Precipitation Evapotranspiration Index (SPEI). The SPI was calculated using the classic standardization approach based on Gamma distribution fitting (McKee et al., 1993). For the SPEI, we followed the methodology of Vicente-Serrano (2010): monthly potential evapotranspiration was estimated using the Thornthwaite model, after which the water surplus values were fitted to a Log-Logistic distribution, and the SPEI values at 3-month and 6-month time

scales were derived through standardization. Detailed calculation procedures for SPI and SPEI are provided in the supplementary material.

To investigate the impacts of extreme climate events on maize yield, we constructed 22 ECIs spanning three categories: five related to extreme high temperature (HD, HSI, AHSD, EDD, HCD), five related to extreme drought (CDD, SPI3, SPI6, SPEI3, SPEI6), and two related to extreme precipitation (R20, CWD) (Table 1). These indices were analyzed across three key growth stages of maize: sowing to jointing, jointing to flowering, and flowering to maturity. Overall, the 22 ECIs were selected based on the actual extreme climate events that maize may encounter during its growth period in the NCP. Their thresholds were determined following the recommendations of the CCI/WCRP/JCOMM Expert Team on Climate Change Detection and Indices (ETCCDI) and relevant studies.

Insert Table 1 here.

2.5 Feature selection

In the feature selection process, two approaches were employed. The first is a linear method, stepwise linear regression (SR), which eliminates redundant predictors and identifies the minimal set of variables that yields optimal linear regression performance. The second is a nonlinear method, the genetic algorithm (GA), used to select the most informative predictors. GA is an optimization algorithm inspired by Darwinian natural selection and genetic mechanisms, designed to simulate biological evolution (Canete et al., 2021). It searches for optimal solutions by mimicking natural evolutionary processes: an initial population of candidate solutions (individuals) is first generated, and new solutions (offspring) are then iteratively produced through mutation, crossover, and selection operations based on a predefined fitness function, continuing until termination criteria are met.

2.6 Machine learning algorithms

Two machine learning algorithms–Random Forest (RF) and Light Gradient Boosting Machine (LGBM) were adopted to improve the ability of the APSIM model to simulate the effects of extreme climatic events on maize yield. RF is a robust ensemble learning technique that builds multiple decision trees and combines their predictions for regression tasks, which significantly enhances predictive performance. This algorithm demonstrates strong resilience against overfitting, high-

dimensional data, missing entries, and outliers (Fan et al., 2024a). As a dependable machine learning approach, RF generates accurate and stable predictions via decision-tree-based ensemble learning (Breiman et al., 2001). Furthermore, it offers an effective way to assess the importance of input variables. The 'randomForest' package in R was employed to implement the RF algorithm, with two critical parameters taken into account: ntree (the number of trees grown in the forest) and mtry (the number of predictor variables randomly sampled at each node).

LGBM is an open-source, high-performance, efficient, and distributed gradient boosting framework that employs a leaf-wise tree growth strategy for constructing decision trees. By leveraging the histogram principle, it converts continuous feature values into discrete bins, thereby reducing memory usage and computational expenses, while also accelerating training speed. Unlike the level-wise decision tree construction method, LGBM builds trees using a depth-constrained leaf-wise growth strategy. This approach avoids unnecessary and overly complex tree structures, reduces ineffective computations, and lowers the risk of overfitting, all of which contribute to higher prediction accuracy. In addition, LGBM integrates two optimization techniques: Gradient-based One-Side Sampling (GOSS) and Exclusive Feature Bundling (EFB). These techniques enable dual dimensionality reduction—both in data volume and feature dimensions, without compromising prediction accuracy, thereby further decreasing the computational cost during model training (Ke et al., 2017). The LGBM method was implemented using the 'lightgbm' package in the R programming language, with four key parameters specified: num_leaves (maximum number of leaves in a decision tree), learning_rate, num_iterations (number of boosting iterations), and max_depth (maximum depth of the tree model). The RF and LGBM models were constructed using five-fold cross-validation with three replications. The final optimal model parameters were selected as the combination that yielded the minimum prediction error.

2.7 Construction and evaluation of hybrid models

The workflow is illustrated in Fig. 2. First, the APSIM-maize model is calibrated and validated using observed phenological and yield data. The implemented model is then run to simulate maize phenology, biomass, and yield. Based on the phenological data outputs, 22 extreme climate indicators across three growth stages are calculated. Next, two methods, SR (and GA), were applied to select the most informative indicators. Finally, the biomass simulated by APSIM and the feature-

selected indicators are used as predictors, which are input into the RF or LGBM to estimate maize yield. Overall, six hybrid models are constructed: RF with SR-selected indicators (APSIM+RF+SR), with GA-selected indicators (APSIM+RF+GA) and with all indicators (APSIM+RF+All); and LGBM with SR-selected indicators (APSIM+LGBM+SR), with GA-selected indicators (APSIM+LGBM+GA) and with all indicators (APSIM+LGBM+All). The performance of the models is quantitatively evaluated using the coefficient of determination (R^2), root mean square error (RMSE), and mean absolute error (MAE), as defined by the following equations:

$$R^2 = \left(\frac{\sum_{i=1}^{n} (O_i - \overline{O})(S_i - \overline{S})}{\sqrt{\sum_{i=1}^{n} (O_i - \overline{O})^2} \sqrt{\sum_{i=1}^{n} (S_i - \overline{S})^2}} \right)^2 \quad (3)$$

$$RMSE = \sqrt{\frac{[\sum_{i=1}^{n} (O_i - S_i)^2]}{n}} \quad (4)$$

$$MAE = \frac{1}{n} \sum_{i=1}^{n} |S_i - O_i| \quad (5)$$

Where n denotes the number of samples, O_i and S_i represent the observed value and simulated value respectively, and $\overline{O}$ and $\overline{S}$ refer to the mean values of the observed values and simulated values. Generally, model performance is considered superior when the coefficient of determination (R^2) approaches 1, and both the mean absolute error (MAE) and root mean square error (RMSE) approach 0.

Insert Fig. 2 here.

3. Results

3.1 APSIM-maize model validation

Overall, the flowering and maturity dates simulated by the APSIM-maize model demonstrated strong agreement with the observed values (Fig. S1a,b,d,e). The RMSE between simulated and observed dates for both phenological stages was less than 5 d. Similarly, the simulated grain yield aligned well with the observed data. The model explained 64% of the yield variability for spring maize and 68% for summer maize, with RMSE values below 20% of the observed yields (Fig. S1c,f).

Discrepancies between simulated and observed yield can be primarily attributed to factors not accounted for in the model, such as pest and disease damage and extreme climate events.

3.2 Hybrid model performance

Feature selection techniques were employed to identify the most relevant predictors for yield estimation from a pool of ECIs. For spring maize, the SR analysis identified an optimal linear model using 10 out of 22 ECIs, which provided the best fit for yield estimation (Table. S3). The selected indices included HD_JF, HD_FM, R20_FM, CDD_FM, CDD_JF, CWD_FM, HD_SJ, CDD_SJ, EDD_JF, and CWD_SJ . In comparison, the GA, which builds a nonlinear regression model, achieved the lowest external RMSE using 12 ECIs: HD_FM, R20_FM, HD_JF, CDD_JF, HD_SJ, CWD_FM, CDD_SJ, HIS_FM, EDD_FM, SHSD_JF, CDD_FM, and EDD_JF (Table. S4). For summer maize, the SR method selected a different set of 10 ECIs for the best-fitting linear model: CDD_JF, HD_FM, R20_JF, CWD_FM, EDD_FM, HIS_FM, HD_JF, AHSD_JF, EDD_JF, and HCD_JF (Table. S5). Meanwhile, the GA model achieved the lowest external RMSE using 12 ECIs, namely R20_JF, HD_FM, EDD_FM, CWD_FM, CDD_JF, HIS_FM, R20_FM, CDD_FM, HD_SJ, EDD_SJ, R20_SJ, and CWD_SJ (Table. S6). These results demonstrate that while both SR and GA are effective for feature selection, the optimal predictors and model complexity vary between spring and summer maize, with the nonlinear GA approach generally yielding higher prediction accuracy.

The APSIM model was further enhanced by integrating feature selection and machine learning algorithms to develop hybrid models for maize yield estimation. All six hybrid models consistently outperformed the standalone APSIM model. For spring maize, the hybrid models based on RF and LGBM explained 92–94% and 83–89% of the observed yield variability, respectively. Compared with the original APSIM simulations, the explained variance increased by 28–30% for RF and 19–25% for LGBM; the MAE decreased by 787.4–846.3 kg ha^{-1} and 595.6–708.6 kg ha^{-1}, and the RMSE decreased by 639.8–846.0 kg ha^{-1} and 392.1–761.7 kg ha^{-1}, respectively (Fig. 3). For summer maize, the RF- and LGBM-based hybrid models explained 91–95% and 81–87% of the observed yield variability, respectively. Relative to the standalone APSIM simulations, the explained variance improved by 27–31% for RF and 17–23% for LGBM; the MAE declined by 612.6–702.0 kg ha^{-1} and 451.9–510.2 kg ha^{-1}, and the RMSE was reduced by 582.2–702.8 kg ha^{-1} and 383.6–512.5 kg ha^{-1}, respectively (Fig. 3). Overall, observed yields ranged from 3689.3. kg ha^{-1}

to 6739.6 kg ha^{-1}, exhibiting considerable interannual variability. While all models captured the temporal dynamics of the observed yields, the APSIM model tended to overestimate actual yields (Fig. S2). This overestimation is primarily attributable to the model's underestimation of the impacts of extreme climate events on maize productivity.

Insert Fig. 3 here.

In terms of the importance of predictors for maize yield estimation, the ranking and selection of ECIs varied among different hybrid models (Fig. S3). For spring maize, applying the SR-screened dataset to the RF model yielded estimation accuracy comparable to APSIM+RF+All. However, the coefficient of determination for APSIM+LGBM+SR (R^2=0.92) was slightly lower than that of APSIM+LGBM+All (R^2=0.95) (Fig. 3a,d,e). In APSIM+RF+SR, the most important predictors were HD_JF, HD_FM, R20_FM, and CDD_FM; in APSIM+LGBM+SR, HD_JF remained the most important, followed by R20_FM, CDD_JF, and CDD_SJ (Fig. S3b). When GA-screened variables were used, the RF model's prediction accuracy was only 0.1 lower than APSIM+RF+All, while APSIM+LGBM+GA (R^2=0.88) was slightly lower than APSIM+LGBM+All (R^2=0.89) (Fig. 3c,f). The top five predictors in APSIM+RF+GA were HD_FM, R20_FM, HD_JF, CDD_JF, and HD_FJ; in APSIM+LGBM+GA, the top four were HD_JF, HD_FM, R20_FM, and CDD_JF (Fig. S3c).

For summer maize, applying the SR-screened dataset to the RF model also produced accuracy comparable to APSIM+RF+All, whereas APSIM+LGBM+SR (R^2 = 0.91) showed a slight decrease compared to APSIM+LGBM+All (R^2=0.95) (Fig. 3j, k). In APSIM+RF+SR, the most important predictors were CDD_JF, HD_FM, R20_JF, and CWD_FM; in APSIM+LGBM+SR, CDD_JF was also the most important, followed by HD_FM, R20_JF, EDD_FM, and HIS_FM (Fig. S3e). When GA-screened variables were applied, the RF model's accuracy was only 0.2 lower than APSIM+RF+All, while APSIM+LGBM+GA (R^2=0.85) was slightly lower than APSIM+LGBM+All (R^2=0.87) (Fig. 3j,l). The top five predictors in APSIM+RF+GA were R20_JF, HD_FM, EDD_FM, CWD_FM, and CDD_JF; in APSIM+LGBM+GA, the top four were HD_FM, R20_JF, CDD_JF, and EDD_FM (Fig. S3f).

Overall, the RF model consistently outperformed the LGBM model across different input feature combinations. The APSIM+RF+GA model achieved R^2 values of 0.94 and 0.93 for spring and summer maize, respectively, demonstrating robust predictive performance. Compared with the

APSIM+RF+All model, its R^2 decreased by only 0.01 for spring maize and 0.02 for summer maize, indicating that the GA-based feature selection maintained high accuracy while using fewer predictor variables. Given its parsimony and strong performance, the APSIM+RF+GA model was selected to project future maize yields in this study.

3.3 Projections of extreme climate indices

Climate warming accelerates maize development, thereby shortening its growth period and leading to substantial changes in extreme climate events during critical phenological stages. In this study, the flowering and maturity dates of maize are projected to be significantly earlier under future climate scenarios (Fig. S4). This study presents the projected changes in 10 extreme climate indices—selected by the genetic algorithm (GA) for spring maize—under different future scenarios (Fig. 4). During the key growth stages of spring maize, all temperature-related indices, including HD_FM, HD_JF, and EDD_FM, exhibit a significant increasing trend across future scenarios (Fig. 4d,c,i). Under the SSP245 scenario, HD_FM and HD_JF are projected to increase by 0.6–1.2 d and 0.5–1.0 d, respectively, with the ranges expanding to 1.0–1.8 d and 0.9–1.5 d under SSP585. EDD_FM is expected to rise by 0.2–0.4°C under SSP245 and 0.3–0.6°C under SSP585, with the most pronounced increase occurring in the SSP585_2080s period. In contrast, changes in precipitation-related indices such as CDD_FM and CWD_FM demonstrate marked scenario dependence. Under SSP245_2040s, CDD_FM increases by 1.0–1.8 d, while under SSP585_2080s, the increase reaches 2.2–3.0 d. CWD_FM shows an increase of 0.8–1.5 d under SSP585_2080s, and R20_FM rises by 0.3–0.7 d under the SSP585 scenario (Fig. 4k,f,b). HD_SJ increases by 0.3–0.6 d under SSP245_2040s and by 1.1–1.7 d under SSP585_2080s, while CDD_SJ rises by 0.5–1.0 d under SSP245 and 1.2–2.1 d under SSP585 (Fig. 4e,d).

Insert Fig. 4 here.

For summer maize, all temperature-related indices during key growth stages—including HD_FM, EDD_FM, and HIS_FM—exhibit significant increasing trends across future scenarios (Fig. S5). Specifically, HD_FM is projected to increase by 0.6–1.1 d under SSP245, with the increase broadening to 1.0–1.7 d under SSP585 (Fig. S5b). EDD_FM rises by 0.2–0.4°C under SSP245 and 0.3–0.6°C under SSP585, with the most pronounced increase occurring in the SSP585_2080s period (Fig. S5c). Precipitation-related indices such as CDD_FM, CWD_FM, and

R20_FM display pronounced scenario-dependent variations (Fig. S5h,l,g). Under SSP245_2040s, CDD_FM increases by 1.0–1.8 d, escalating to 2.2–3.0 d under SSP585_2080s. CWD_FM shows an increase of 0.8–1.5 d under SSP585_2080s, while R20_FM rises by 0.3–0.7 d under SSP585. HD_SJ increases by 0.3–0.6 d under SSP245_2040s, with the range expanding to 1.1–1.7 d under SSP585_2080s. CDD_JF rises by 0.5–1.0 d under SSP245 and 1.2–2.1 d under SSP585 (Fig. S5i,e).

3.4 Comparison of APSIM model and hybrid model for projecting future maize yield

During the baseline period (1981–2010), the spring and summer maize yields simulated by the APSIM+RF+GA model were slightly lower than those simulated by the standalone APSIM model (Fig. 5). Based on the arithmetic mean of multiple GCMs, both models project a declining trend in maize yields across the NCP under future climate scenarios relative to the baseline period. Overall, both the APSIM and APSIM+RF+GA models projected greater declines in simulated yields under higher emission scenarios. Under the scenario without CO_2 fertilization effects, and compared with the respective baseline yields, the spring maize yield reductions simulated by the APSIM and APSIM+RF+GA models were 21.0% and 19.5% under SSP245_2080s, respectively, with these reductions expanding to 40.1% and 43.6% under SSP585_2080s (Fig. 5a). For summer maize, the corresponding yield reductions were 17.0% and 17.2% under SSP245_2080s, and 25.0% and 26.8% under SSP585_2080s (Fig. 5b).

Insert Fig. 5 here.

Under the scenario with CO_2 fertilization effects, the yield reductions projected by both models were substantially smaller than those under the without CO_2 scenario, with the divergence between the with and without CO_2 scenarios widening under higher emission scenarios (Fig. 5). Compared with the baseline yields simulated by the respective models, for spring maize, the yield reductions simulated by the APSIM and APSIM+RF+GA models narrowed to 6.3% and 8.5%, respectively, under the SSP245_2080s scenario with CO_2 fertilization, and narrowed to 22.1% and 25.9% under the SSP585_2080s scenario (Fig. 5a). For summer maize, the yield reductions were 15.2% and 14.6% under SSP245_2080s with CO_2 fertilization, and 16.2% and 24.6% under SSP585_2080s (Fig. 5b). CO_2 fertilization effects significantly alleviate the negative impacts of future climate warming on maize yields. Notably, the APSIM+RF+GA hybrid model, which incorporates the effects of extreme

climate events, consistently projected larger yield reductions than the standalone APSIM model across all scenarios (Fig. 5).

Based on the simulations from the APSIM model and the APSIM+RF+GA hybrid model at 51 stations across NCP, maize yield changes under future climate scenarios exhibit significant spatial heterogeneity and inter-model differences (Fig. 6, Fig. S6). When CO_2 fertilization effects are considered, the APSIM model projects that under the SSP245_2040s scenario, yields at 10 out of 51 stations show slight increases, while yields at all remaining stations exhibit declining trends. Under the SSP585_2080s scenario, all 51 stations show yield declines, with 14 stations experiencing reductions exceeding 20%. Simulation results from the APSIM+RF+GA model indicate that under the SSP245_2040s scenario, all but three stations show yield reductions. Under the SSP585_2080s scenario, yields at 9 out of 51 stations decline by more than 35%. From a temporal perspective, both the APSIM and APSIM+RF+GA models project that yield reductions for spring and summer maize will be substantially larger in the 2080s compared to the 2040s, with the most severe declines occurring under the SSP585 scenario.

Insert Fig. 6 here.

4. Discussion

4.1 Performance and advantages of the hybrid models

In this study, the applicability of the APSIM model for simulating maize growth in the NCP was systematically evaluated. The results showed that the model simulated the key phenological stages and grain yield of maize with acceptable accuracy, explaining 64% and 68% of the historical yield variability for spring and summer maize, respectively, with simulation errors consistently within 20% of the observed values. These performance metrics align closely with validation results from similar studies, indicating that the APSIM model reasonably captures the biophysical processes governing maize growth under conventional climatic conditions in the NCP (Bai et al., 2024). However, the model exhibited systematic overestimation of yield in certain years, particularly those marked by frequent extreme climate events. This bias is largely attributable to its simplified representation of stress mechanisms associated with extreme weather (Li et al., 2023a). Although APSIM accounts for the effects of temperature and water stress on photosynthesis, it

insufficiently quantifies critical processes such as heat-induced pollen sterility and pollination failure, nor does it simulate waterlogging stress resulting from extreme precipitation. Moreover, the model excludes biotic stress factors—such as pest and disease pressures—that often interact synergistically with climatic stressors under field conditions (Kephe et al., 2021). These limitations suggest that relying exclusively on APSIM to assess climate change impacts, particularly under future scenarios with increased frequency and intensity of extreme events, may not fully capture the potential risks of maize yield reduction.

To address these gaps, this study developed a hybrid simulation framework that couples the process-based APSIM model with machine learning algorithms, specifically RF and LGBM. This integrated approach substantially improved the accuracy of maize yield simulations across the NCP, especially under extreme climatic conditions. Compared to the standalone APSIM model, the APSIM+RF+GA framework increased the R^2 values for historical yield variability by 28–30% for spring maize and 27–31% for summer maize, while also significantly reducing the MAE and RMSE. This performance enhancement stems from two key advantages. First, APSIM provides a robust process-based foundation for simulating fundamental biophysical processes, including crop phenology, biomass accumulation, and the dynamics of water and nitrogen (Yadav et al., 2025). Second, machine learning algorithms—particularly RF—effectively capture the nonlinear responses and complex interactions induced by extreme climate events, which are not yet fully represented in APSIM (Nouri et al., 2025). The integration of a GA further refined model inputs, mitigating the risks of the curse of dimensionality and overfitting while preserving high predictive accuracy. Previous studies have similarly demonstrated that GA-based feature selection can enhance model performance using a minimal set of informative predictors (Ding et al., 2025). Our results further indicate that the APSIM+RF model, constructed with predictor variables selected by the GA, explains 94% and 93% of the yield variation for spring and summer maize, respectively. This configuration achieves an optimal balance between predictive accuracy and computational efficiency, highlighting its potential as a reliable tool for assessing maize yield responses under future climate scenarios.

4.2 Changes in extreme climate indices (ECIs) and its impacts on maize yield in future

Under global warming, both spring and summer maize in the NCP face intensifying extreme climate stress, albeit with distinct response characteristics. Extreme high temperature events for both maize types increase significantly with higher emission intensities and over time. This increase during the jointing–flowering period is primarily attributed to climate warming-induced advances in crop phenology, with summer maize exhibiting a more pronounced trend (Wei et al., 2020). These temperature extremes critically constrain yield formation through distinct mechanisms. Around the jointing stage, extreme high temperatures directly inhibit leaf photosynthesis and enhance respiratory consumption, reducing ear number per unit area and potential grain number per ear (Fan et al., 2024b). During the flowering stage, extreme high temperatures impair pollen viability, accelerate filament senescence, and obstruct pollination and fertilization, leading to marked reductions in grain number per ear (Li et al., 2025).

Drought stress shows slight alleviation during the flowering–maturity stage under medium-low emission scenarios (excluding SSP585_2080s), with some studies indicating a decreasing trend in extreme drought events across the NCP (Xu et al., 2024). However, for summer maize, extreme drought at the jointing stage remains a primary constraint on yield formation (Qi et al., 2022). Although drought events occur with higher frequency for spring maize, their relative impact on yield is lower compared to extreme temperature and rainfall, partly due to effective mitigation through irrigation (Ma et al., 2022).

Extreme rainfall events exhibit significant spatiotemporal heterogeneity. Under high emission scenarios, extreme rainfall increases during specific growth stages, potentially inducing waterlogging risk, while changes remain relatively moderate under medium-low emission scenarios. This uneven rainfall distribution increases the probability of crops experiencing periodic drought or waterlogging, thereby elevating maize production risks (Liu et al., 2022). During the flowering stage, extreme or continuous rainfall disrupts pollination by washing away pollen, inhibiting anther dehiscence, and increasing field humidity (Dong et al., 2023). Concurrently, waterlogging induces root hypoxia, weakens nutrient uptake, and promotes pest and disease incidence, reducing grain weight and biomass accumulation (Zhang et al., 2025).

Overall, future changes in extreme weather events will substantially increase climate risks for maize production, with long-term risks under high emission scenarios being particularly prominent.

The differential responses of spring and summer maize to various extreme stressors-spring maize is mainly threatened by extreme high temperatures and extreme rainfall during the flowering–maturity stage, while summer maize is constrained by drought during the jointing–flowering stage and high temperatures around the flowering stage—highlighting the need for crop-specific adaptation strategies to mitigate future yield losses.

4.3 The CO_2 fertilization effect in maize yield projections

In this study, the yield predictions of maize under future climate scenarios in the NCP were compared with and without considering the CO_2 fertilization effect. Across all future climate scenarios, model simulations consistently showed a decreasing trend in maize production. However, compared to simulations without CO_2, the projected yield reductions were significantly smaller when the CO_2 fertilization effect was considered, and this mitigating effect was more pronounced under high emission scenarios. For example, under the SSP585_2080 scenario without CO_2, spring maize yield decreased by 40.1% and summer maize by 25.0%. After incorporating the CO_2 fertilization effect, the reductions were only 22.1% for spring maize and 16.2% for summer maize. This compensatory effect occurs because elevated CO_2 enhances photosynthetic rate and carbon assimilation capacity, thereby alleviating yield loss (Allen et al., 2011). However, as a typical C_4 crop, maize differs fundamentally from C_3 crops in photosynthetic metabolism and CO_2 response mechanisms. Consequently, the yield-enhancing effect of CO_2 becomes significantly limited—or even disappears—when concentrations are excessively high (Li et al., 2023b). Furthermore, high CO_2 concentrations can accelerate maize phenological development. The resulting shortened growth period reduces the duration for dry matter accumulation, particularly when high temperatures coincide with the grain-filling stage, increasing the risk of insufficient grain filling and ultimately offsetting potential yield gains (Cairns et al., 2013).

Notable differences were observed between the yield simulations of the standalone APSIM model and the coupled APSIM+RF+GA model for both spring and summer maize, regardless of whether the CO_2 fertilization effect was considered. Taking the SSP585_2080s scenario as an example, without CO_2 fertilization, the standalone APSIM projected yield reductions of 40.1% for spring maize and 25.0% for summer maize, whereas the coupled model projected reductions of 43.6% and 26.8%, respectively. When CO_2 fertilization was considered, the standalone APSIM projected

reductions of 22.1% for spring maize and 16.2% for summer maize, while the coupled model projected reductions of 25.0% and 24.6%, respectively. The standalone APSIM model failed to fully capture the nonlinear stress effects of extreme high temperatures and drought events on crop growth during key phenological stages, leading to an overestimation of future yields (Bai et al., 2024). Previous studies have largely relied on crop models coupled with General Circulation Models (GCMs) to assess future maize yields (Zhao et al., 2022). These approaches may have underestimated the impacts of extreme climate events on crop productivity, resulting in overly optimistic projections. Appropriate agronomic adaptations—such as adjusting sowing dates and breeding stress-resistant varieties—can help mitigate or avoid the adverse effects of extreme climate events. Future research should prioritize the use of hybrid models that integrate comprehensive crop models with machine learning algorithms to explore adaptation strategies under increasingly extreme climate conditions.

5 Conclusion

This study developed a hybrid framework coupling the APSIM process-based model with machine learning (RF and LGBM) and feature selection (SR and GA). The APSIM+RF+GA model performed best, explaining 94% and 93% of spring and summer maize yield variations, improving simulation accuracy by over 30% compared to APSIM alone, and effectively addressing the limitations of traditional models in capturing extreme climate impacts.

Key findings indicate that extreme high temperature during flowering–grain filling for spring maize and extreme drought during jointing–flowering for summer maize are critical impact factors. Under future scenarios, all extreme temperature indices show rising trends, with yield losses significantly higher under SSP585 than SSP245 and more severe in the 2080s than 2040s, particularly in the central and southeastern plain. The CO_2 fertilization effect cannot fully offset these negative impacts. The hybrid model reveals greater yield reduction risks than APSIM alone, suggesting standalone process-based models may underestimate future climate risks, providing a scientific basis for targeted adaptation strategies.

Reference

Allen L H, Kakani V G, Vu J C V, Boote K J (2011) Elevated CO_2 increases water use efficiency by

sustaining photosynthesis of water-limited maize and sorghum. Journal of Plant Physiology, 168(16), 1909–1918. https://doi.org/10.1016/j.jplph.2011.05.005

Bai H Z, Xiao DP, Tang J, Liu DL (2024) Evaluation of wheat yield in North China Plain under extreme climate by coupling crop model with machine learning. Computers and Electronics in Agriculture, 217, 108651. https://doi.org/10.1016/j.compag.2024.108651

Breiman L (2001) Random Forests. Machine Learning, 45(1), 5–32. https://doi.org/10.1023/A:1010933404324

Cairns J E, Hellin J, Sonder K, Araus J L, MacRobert J F, Thierfelder C, Prasanna B M (2013) Adapting maize production to climate change in sub-Saharan Africa. Food Security, 5(3), 345–360. https://doi.org/10.1007/s12571-013-0256-x

Ding J, Du J, Wang H, Xiao S (2025) A novel two-stage feature selection method based on random forest and improved genetic algorithm for enhancing classification in machine learning. Scientific Reports, 15(1), 16828. https://doi.org/10.1038/s41598-025-01761-1

Dong M, Zhao J, Li E, Liu Z, Guo S, Zhang Z, Cui W, Yang X (2023) Effects of Changing Climate Extremes on Maize Grain Yield in Northeast China. Agronomy, 13(4), 1050. https://doi.org/10.3390/agronomy13041050

Erfanian S, Zhou Y, Razzaq A, Abbas A, Safeer A A, Li T (2022) Predicting Bitcoin (BTC) Price in the Context of Economic Theories: A Machine Learning Approach. Entropy, 24(10), 1487. https://doi.org/10.3390/e24101487

Fan X, Hu X, Ma Y, Pang Y, Sun J, Hou P (2024) Influence of high temperature and drought stress at jointing stage on crop physiological responses and growth in summer maize plants (Zea mays L.). Frontiers in Plant Physiology, 2, 1331421. https://doi.org/10.3389/fphgy.2024.1331421

Fan Y (2024). Research on Data Asset Feature Analysis and Value Evaluation Strategy Based on Random Forest and B-P Neural Network. Academic Journal of Business Management, 6(11). https://doi.org/10.25236/AJBM.2024.061107

Feng P, Wang B, Liu D L, Waters C, Xiao D, Shi L, Yu Q (2020) Dynamic wheat yield forecasts are improved by a hybrid approach using a biophysical model and machine learning technique. Agricultural and Forest Meteorology, 285–286, 107922. https://doi.org/10.1016/j.agrformet.2020.107922

Feng P, Wang B, Liu D L, Waters C, Yu Q (2019) Incorporating machine learning with biophysical model can improve the evaluation of climate extremes impacts on wheat yield in south-eastern Australia. Agricultural and Forest Meteorology, 275, 100–113. https://doi.org/10.1016/j.agrformet.2019.05.018

Fernandez de Canete J, del Saz-Orozco P, Gómez-de-Gabriel J, Baratti R, Ruano A, Rivas-Blanco I (2021) Control and soft sensing strategies for a wastewater treatment plant using a neuro-genetic approach. Computers Chemical Engineering, 144, 107146. https://doi.org/10.1016/j.compchemeng.2020.107146

Fu, Z Z, Zhu G X, Liu Z J, Guo, S B, Li E, Yang, X G (2023) Spatial-Temporal Variations of High Temperature During Flowering Period in Maize-Producing Areas of China Under Climate Change. Scientia Agricultura Sinica, 56(14), 2686–2700. https://doi.org/10.3864/j.issn.0578-1752.2023.014.005

GB/T 20481-2017 (2017) Grades of Meteorological Drought. Standardization Administration of the People's Republic of China: Beijing, China.

Holzworth D P, Huth N I, deVoil P G, Zurcher E J, Herrmann N I, McLean G, Chenu K, Van Oosterom E J, Snow V, Murphy C, Moore A D, Brown H, Whish J P M, Verrall S, Fainges J, Bell L W, Peake A S, Poulton P L, Hochman Z, et al (2014) APSIM – Evolution towards a new generation of agricultural systems simulation. Environmental Modelling Software, 62, 327–350. https://doi.org/10.1016/j.envsoft.2014.07.009

Hu T, Zhang X, Khanal S, Wilson R, Leng G, Toman E M, Wang X, Li Y, Zhao K (2024) Climate change impacts on crop yields: A review of empirical findings, statistical crop models, and machine learning methods. Environmental Modelling Software, 179, 106119. https://doi.org/10.1016/j.envsoft.2024.106119

Intergovernmental Panel On Climate Change (IPCC) (2023) Climate Change 2022 – Impacts, Adaptation and Vulnerability: Working Group II Contribution to the Sixth Assessment Report of the Intergovernmental Panel on Climate Change (1st ed.). Cambridge University Press. https://doi.org/10.1017/9781009325844

Jahangirlou M R, Morel J, Akbari G A, Alahdadi I, Soufizadeh S, Parsons D (2023) Combined use of APSIM and logistic regression models to predict the quality characteristics of maize grain. European Journal of Agronomy, 142, 126629. https://doi.org/10.1016/j.eja.2022.126629

Jeong J H, Resop J P, Mueller N D, Fleisher D H, Yun K, Butler E , Timlin, D J, Shim K M, Gerber J S, Reddy V R, Kim S H (2016) Random Forests for Global and Regional Crop Yield Predictions. PLOS ONE, 11(6), e0156571. https://doi.org/10.1371/journal.pone.0156571

Ji C, Agathokleous E, Ju L, Yu Z, Zhu X, Jiang T, Su B, Wang G, Tao S, Miao L, Sun S, Liu Q (2025) Growing threat of climate-induced abrupt dry-wet transitions in Northern China. Atmospheric Research, 326, 108325. https://doi.org/10.1016/j.atmosres.2025.108325

Jiang Y, Zhao L, Li X, Chen X, Zou X, Wang Y, Zeng H, Cui T, Zhong H (2025) State of China's climate in 2024. Atmospheric and Oceanic Science Letters, 18(5), 100661. https://doi.org/10.1016/j.aosl.2025.100661

Ke G, Meng Q, Finley T, Wang T, Chen W, Ma W, Ye Q, Liu T-Y (n.d.) LightGBM: A Highly Efficient Gradient Boosting Decision Tree.

Kephe P N, Ayisi K K, Petja B M (2021) Challenges and opportunities in crop simulation modelling under seasonal and projected climate change scenarios for crop production in South Africa. Agriculture Food Security, 10(1), 10. https://doi.org/10.1186/s40066-020-00283-5

Li J, Li G, Wang L, Li D, Li H, Gao C, Zhuang M, Zhuang J, Zho H, Xu S, Hu Z, Wang E (2023a) Predicting maize yield in Northeast China by a hybrid approach combining biophysical modelling and machine learning. Field Crops Research, 302, 109102. https://doi.org/10.1016/j.fcr.2023.109102

Li Q, Wang P, Li Y, Tang J, Li X, Zhang Y, Han D, Zhao Y, Wang Q, Yang Z (2025) Identifying trigger thresholds for heat damage at different growth stages of summer maize: A case study of the Huang-Huai-Hai Plain, China. European Journal of Agronomy, 170, 127729. https://doi.org/10.1016/j.eja.2025.127729

Li S, Leakey A D B, Moller C A, Montes C M, Sacks E J, Lee D, Ainsworth E A (2023b) Similar photosynthetic but different yield responses of C3 and C4 crops to elevated O3. Proceedings of the National Academy of Sciences, 120(46), e2313591120. https://doi.org/10.1073/pnas.2313591120

Li T, Zhang X, Liu Q, Liu J, Chen Y, Sui P (2022) Yield penalty of maize (Zea mays L.) under heat stress in different growth stages: A review. Journal of Integrative Agriculture, 21(9), 2465–

2476. https://doi.org/10.1016/j.jia.2022.07.013
Li Z, Xu M (2025) The Impact of High Temperature Stress on Maize Reproductive Development and the Regulation Mechanism of Heat Tolerance. Maize Genomics and Genetics. https://doi.org/10.5376/mgg.2025.16.0013
Liu B Y, Lin B J, Li X X, Virk A L, N'dri Yves B, Zhao X, Dang Y P, Zhan H L (2021) Appropriate farming practices of summer maize in the North China Plain: Reducing nitrogen use to promote sustainable agricultural development. Resources, Conservation and Recycling, 175, 105889. https://doi.org/10.1016/j.resconrec.2021.105889
Liu D L, Zuo H (2012) Statistical downscaling of daily climate variables for climate change impact assessment over New South Wales, Australia. Climatic Change, 115(3–4), 629–666. https://doi.org/10.1007/s10584-012-0464-y
Liu W, Li Z, Li Y, Ye T, Chen S, Liu Y (2022) Heterogeneous impacts of excessive wetness on maize yields in China: Evidence from statistical yields and process-based crop models. Agricultural and Forest Meteorology, 327, 109205. https://doi.org/10.1016/j.agrformet.2022.109205
Ma S, Hou J, Wang Y, Wang M, Zhang W, Fan Y, Huang Z (2022) Post-flowering Soil Waterlogging Curtails Grain Yield Formation by Restricting Assimilates Supplies to Developing Grains. Frontiers in Plant Science, 13, 944308. https://doi.org/10.3389/fpls.2022.944308
McKee T B, Doesken N J, Kleist J (n.d.) THE RELATIONSHIP OF DROUGHT FREQUENCY AND DURATION TO TIME SCALES.
NBS (National Bureau of Statistics of China) (2022) International statistical yearbook. China statistics press, Beijing, China.
Nouri M, Veysi S (2025) Mitigating crop modeling uncertainties through machine learning in drylands. Scientific Reports, 15(1), 42663. https://doi.org/10.1038/s41598-025-26811-6
O'Neill B C, Tebaldi C, Van Vuuren D P, Eyring V, Friedlingstein P, Hurtt G, Knutti R, Kriegler E, Lamarque J-F, Lowe J, Meehl G A, Moss R, Riahi K, Sanderson B M (2016) The Scenario Model Intercomparison Project (ScenarioMIP) for CMIP6. Geoscientific Model Development, 9(9), 3461–3482. https://doi.org/10.5194/gmd-9-3461-2016
Patil Y, Fathima R, Sundarajan S, Sridevi Ponmalar P, Ramachandran H (2024) Impact of Feature Selection on Wheat Yield Prediction Using Machine Learning. International Journal of Design Nature and Ecodynamics, 19(6), 1909–1917. https://doi.org/10.18280/ijdne.190607
Qi Y, Zhang Q, Hu S, Wang R, Wang H, Zhang K, Zhao H, Ren S, Yang Y, Zhao F, Chen F, Yang Y (2022) Effects of High Temperature and Drought Stresses on Growth and Yield of Summer Maize during Grain Filling in North China. Agriculture, 12(11), 1948. https://doi.org/10.3390/agriculture12111948
Rajabi Dehnavi A, Zahedi M, Ludwiczak A, Cardenas Perez S, Piernik A (2020) Effect of Salinity on Seed Germination and Seedling Development of Sorghum (Sorghum bicolor (L.) Moench) Genotypes. Agronomy, 10(6), 859. https://doi.org/10.3390/agronomy10060859
Ritchie JT, Kiniry JR, Jones CA, Dyke PT (1986) CERES-Maize: a simulation model of maize growth and development. Texas A&M University Press, College Station
Roberts M J, Braun N O, Sinclair T R, Lobell D B, Schlenker W (2017) Comparing and combining process-based crop models and statistical models with some implications for climate change. Environmental Research Letters, 12(9), 095010. https://doi.org/10.1088/1748-9326/aa7f33
Sajid S S, Shahhosseini M, Huber I, Hu G, Archontoulis S V (2022) County-scale crop yield prediction by integrating crop simulation with machine learning models. Frontiers in Plant

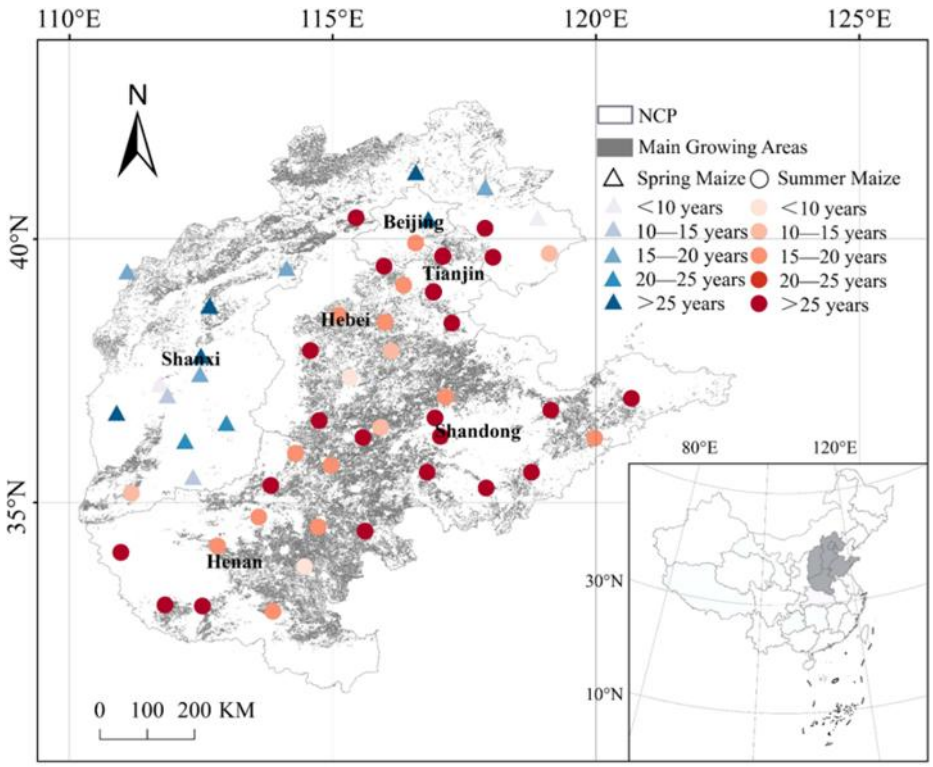
Science, 13, 1000224. https://doi.org/10.3389/fpls.2022.1000224
Shahhosseini M, Hu G, Huber I, Archontoulis S V (2021) Coupling machine learning and crop modeling improves crop yield prediction in the US Corn Belt. Scientific Reports, 11(1), 1606. https://doi.org/10.1038/s41598-020-80820-1
Sutanto S J, Duku C, Gülveren M, Dankers R, Paparrizos S (2025) Future intensification of compound and consecutive drought and heatwave risks in Europe. Natural Hazards and Earth System Sciences, 25(10), 3879–3895. https://doi.org/10.5194/nhess-25-3879-2025
Tang H, Zhang L, Xie X, Wang Y, Wang T, Liu C (2025) Resilience of Maize to Environmental Stress: Insights into Drought and Heat Tolerance. International Journal of Molecular Sciences, 26(11), 5274. https://doi.org/10.3390/ijms26115274
Van Klompenburg T, Kassahun A, Catal C (2020) Crop yield prediction using machine learning: A systematic literature review. Computers and Electronics in Agriculture, 177, 105709. https://doi.org/10.1016/j.compag.2020.105709
Vicente-Serrano S M, Beguería S, López-Moreno J I (2010) A Multiscalar Drought Index Sensitive to Global Warming: The Standardized Precipitation Evapotranspiration Index. Journal of Climate, 23(7), 1696–1718. https://doi.org/10.1175/2009JCLI2909.1
Wang B, Waters C, Orgill S, Cowie A, Clark A, Li Liu D, Simpson M, McGowe I, Sides T (2018) Estimating soil organic carbon stocks using different modelling techniques in the semi-arid rangelands of eastern Australia. Ecological Indicators, 88, 425–438. https://doi.org/10.1016/j.ecolind.2018.01.049
Wei S, Liu J, Li T, Wan, X, Peng A, Chen C (2020) Effect of High-Temperature Events When Heading into the Maturity Period on Summer Maize (Zea mays L.) Yield in the Huang-Huai-Hai Region, China. Atmosphere, 11(12), 1291. https://doi.org/10.3390/atmos11121291
Xiao D P, Bai H Z, Liu D L, Tang J, Wang B, Shen Y, Cao J, Feng P (2022) Projecting future changes in extreme climate for maize production in the North China Plain and the role of adjusting the sowing date. Mitigation and Adaptation Strategies for Global Change, 27(3), 21. https://doi.org/10.1007/s11027-022-09995-4
Xu F, Qu Y, Bento V A, Song H, Qiu J, Qi J, Wan L, Zhang R, Miao L, Zhang X, Wang Q (2024) Understanding climate change impacts on drought in China over the 21st century: A multi-model assessment from CMIP6. Npj Climate and Atmospheric Science, 7(1), 32. https://doi.org/10.1038/s41612-024-00578-5
Yadav B, Krishnan P, Parihar C M, Banerjee K (2025) Modelling crop growth and soil hydrothermal regimes under conservation agriculture using APSIM-wheat. Scientific Reports, 15(1), 36362. https://doi.org/10.1038/s41598-025-20211-6
Zeng R, Lin X, Sassenrath G F, Welch S M, Yao F (2026) Current and projected impacts of extreme climate events on winter wheat yield in Northern China. Communications Earth Environment, 7(1), 100. https://doi.org/10.1038/s43247-025-02954-2
Zhang Y, Chen X, Geng S, Zhang X (2025) A review of soil waterlogging impacts, mechanisms, and adaptive strategies. Frontiers in Plant Science, 16, 1545912. https://doi.org/10.3389/fpls.2025.1545912
Zhao Y, Xiao D, Bai H, Liu D L, Tang J, Qi Y, Shen Y (2022) Climate Change Impact on Yield and Water Use of Rice–Wheat Rotation System in the Huang-Huai-Hai Plain, China. Biology, 11(9), 1265. https://doi.org/10.3390/biology11091265

686 Table 1 Information of 22 extreme climate indices (ECIs) defined in this study.

Index	Definition	Unit	Reference
HD_ SJ	The number of days with Tmax > 34 ℃ from sowing to jointing	d	Ritchie et al. (1986)
HD_ JF	The number of days with Tmax > 34.6 ℃ from jointing to flowering	d	Li et al. (2025)
HD_ FM	The number of days with Tmax > 32.9 ℃ from flowering to maturity	d	Li et al. (2025)
HIS_ FM	The average Tmax for days when > 34°C from 10 days before flowering to 30 days after flowering	℃	Li et al. (2022)
AHSD	The number of days when temperature > 30°C from tasseling to 16 days after tasseling	℃	Fu et al. (2023)
EDD_ SJ	The Tmax is greater than the accumulated temperature of 34° C	℃	SAC (2017)
EDD_ JF	The Tmax is greater than the accumulated temperature of 34.6 °C	℃	SAC (2017)
EDD_ FM	The Tmax is greater than the accumulated temperature of 32.9 °C	℃	SAC (2017)
HCD	The number of days with three or more continuous days of Tmax >34 ℃ from 10 days before flowering to 30 days after flowering	℃	Xiao et al. (2022)
CDD_ SJ	The maximum number of consecutive days with daily precipitation < 5 mm from sowing to jointing	d	ETCCDI
CDD_ JF	The maximum number of consecutive days with daily precipitation < 5 mm from jointing to flowering	d	ETCCDI
CDD_ FM	The maximum number of consecutive days with daily precipitation < 5 mm from flowering to maturity	d	ETCCDI
SPI_3	Taking moderate drought as the benchmark, calculate the SPI for the period from June to August. When SPI3 is lower than -1, it is determined as a meteorological drought event (DSPI3); while if SPI3 exceeds 1, it is determined as an extreme wet event (WSPI3).	-	Li et al. (2023a)
SPI_6	Taking moderate drought as the benchmark, calculate the SPI for the period from March to September. When SPI6 is lower than -1, it is determined as a meteorological drought event (DSPI6); while if SPI6 exceeds 1, it is determined as an extreme wet event (WSPI3).	-	Li et al. (2023a)
SPEI_3	Calculate the SPEI values for the period from June to August. The SPEI values ranging from -1 to -1.5 indicate mild drought, those between -1.5 and -2.0 indicate moderate drought, and values below -2.0 are classified as severe drought.	-	Li et al. (2023a)
SPEI_6	Calculate the SPEI values for the period from March to September. The SPEI values ranging from -1 to -1.5 indicate mild drought, those between -1.5 and -2.0 indicate moderate drought, and values below -2.0 are classified as severe drought.	-	Li et al. (2023a)
R20_SJ	The number of days with daily precipitation ≥ 20 mm from sowing to jointing	d	ETCCDI

R20_ JF	The number of days with daily precipitation ≥ 20 mm from jointing to flowering	d	ETCCDI
R20_ FM	The number of days with daily precipitation ≥ 20 mm from flowering to maturity	d	ETCCDI
CWD_SJ	The maximum number of consecutive days with daily precipitation ≥1 mm from sowing to jointing	d	ETCCDI
CWD_JF	The maximum number of consecutive days with daily precipitation ≥1 mm from jointing to flowering	d	ETCCDI
CWD_FM	The maximum number of consecutive days with daily precipitation ≥1 mm from flowering to maturity	d	ETCCDI

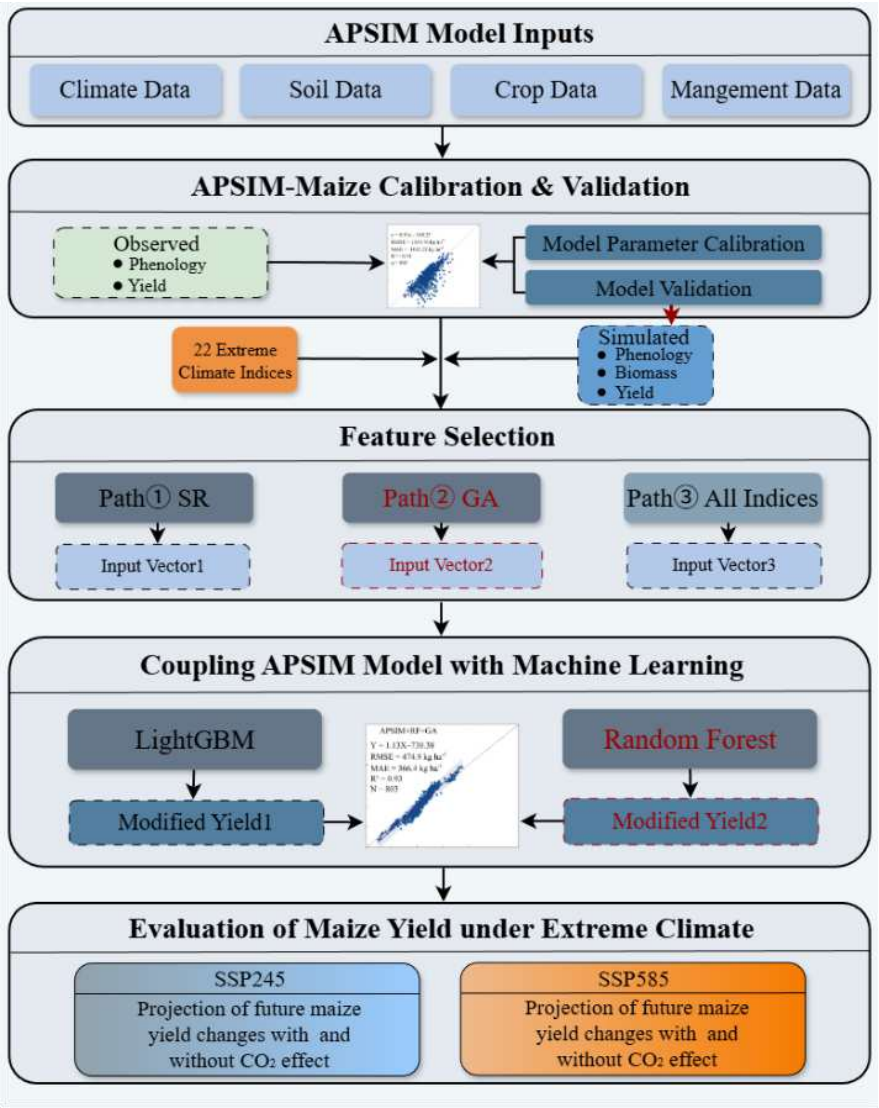
687



688

689 Fig. 1 Location of agricultural meteorological stations for maize in the North China Plain. Color

690 gradients for triangles and circles indicate years of available observational data record at each station.



691

692 Fig. 2 Flowchart of the procedures used in this study, where SR, GA, RF and LGBM were step-wise

693 regression, genetic algorithm, LightGBM and random forest, respectively.

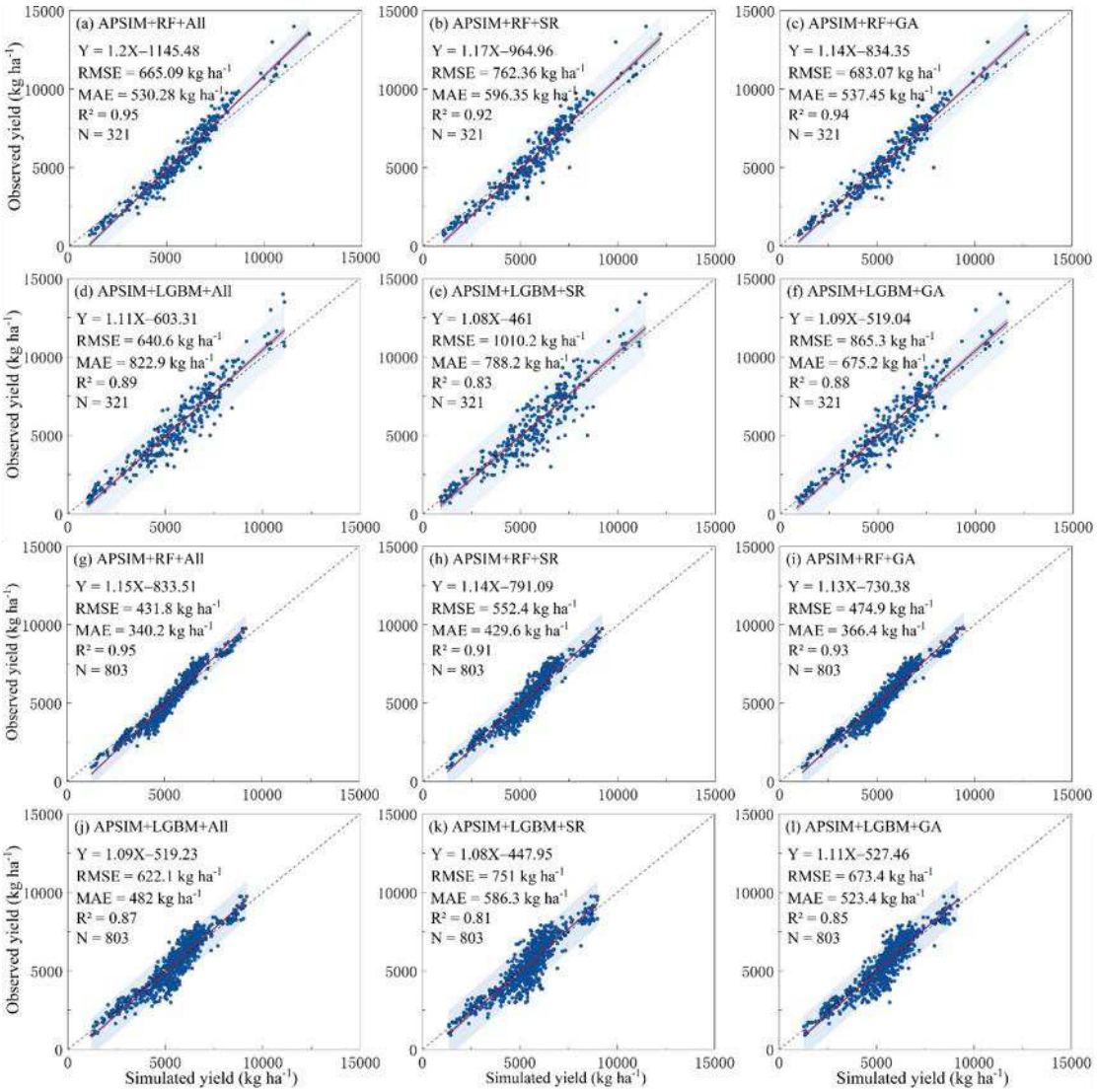
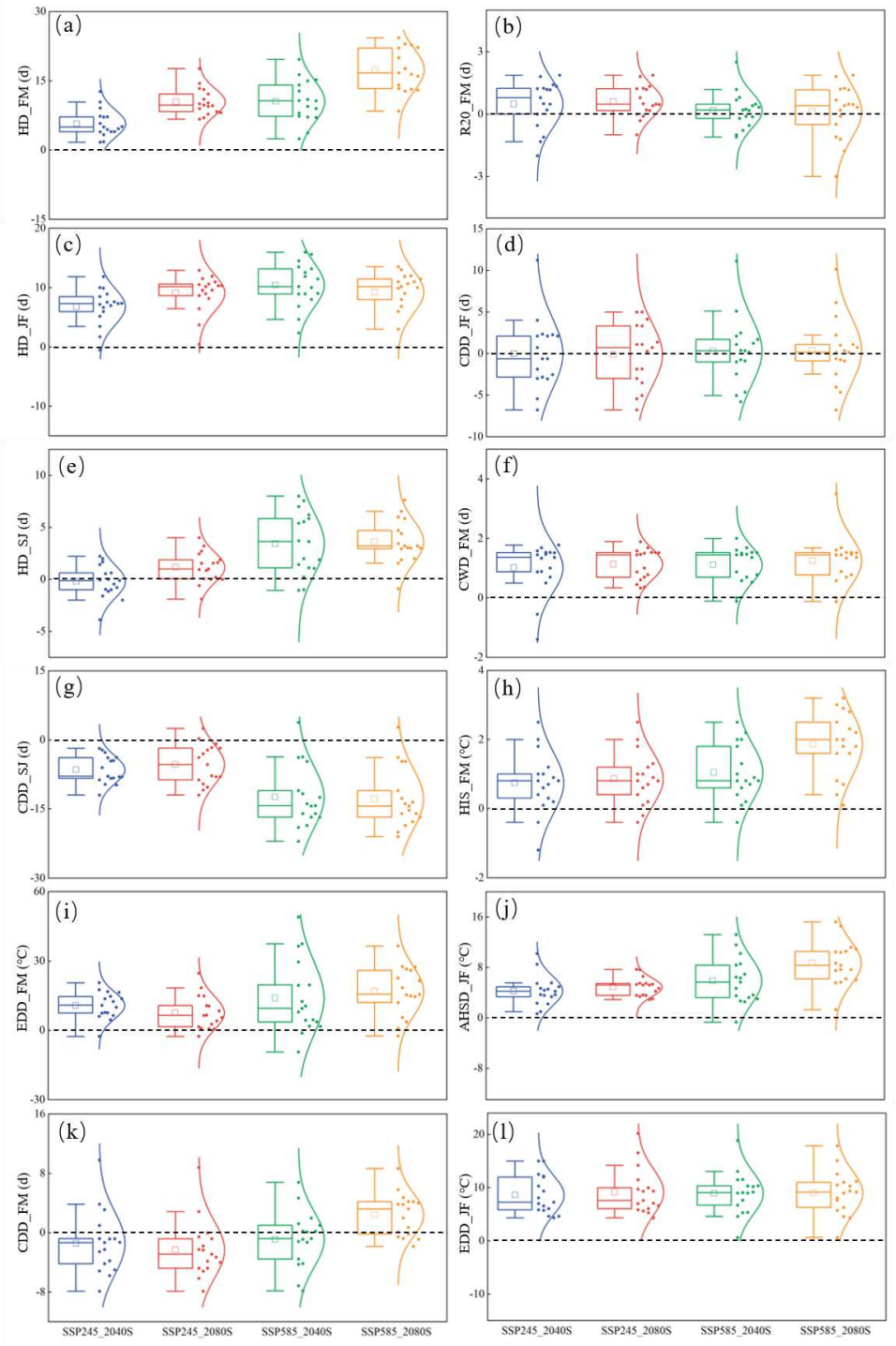


Fig. 3 Comparison of observed and simulated spring (a-f) and summer (g-i) maize yields using RF and LGBM with all predictors, SR (10 out of 22 predictors selected by stepwise regression method) and GA (12 out of 22 predictors selected by genetic algorithms).



699

700 Fig. 4 Projected changes in 12 extreme climate indices (ECIs) selected by GA for spring maize in

701 the 2040s and 2080s under SSP245 and SSP585 scenarios compared to the baseline period.

702

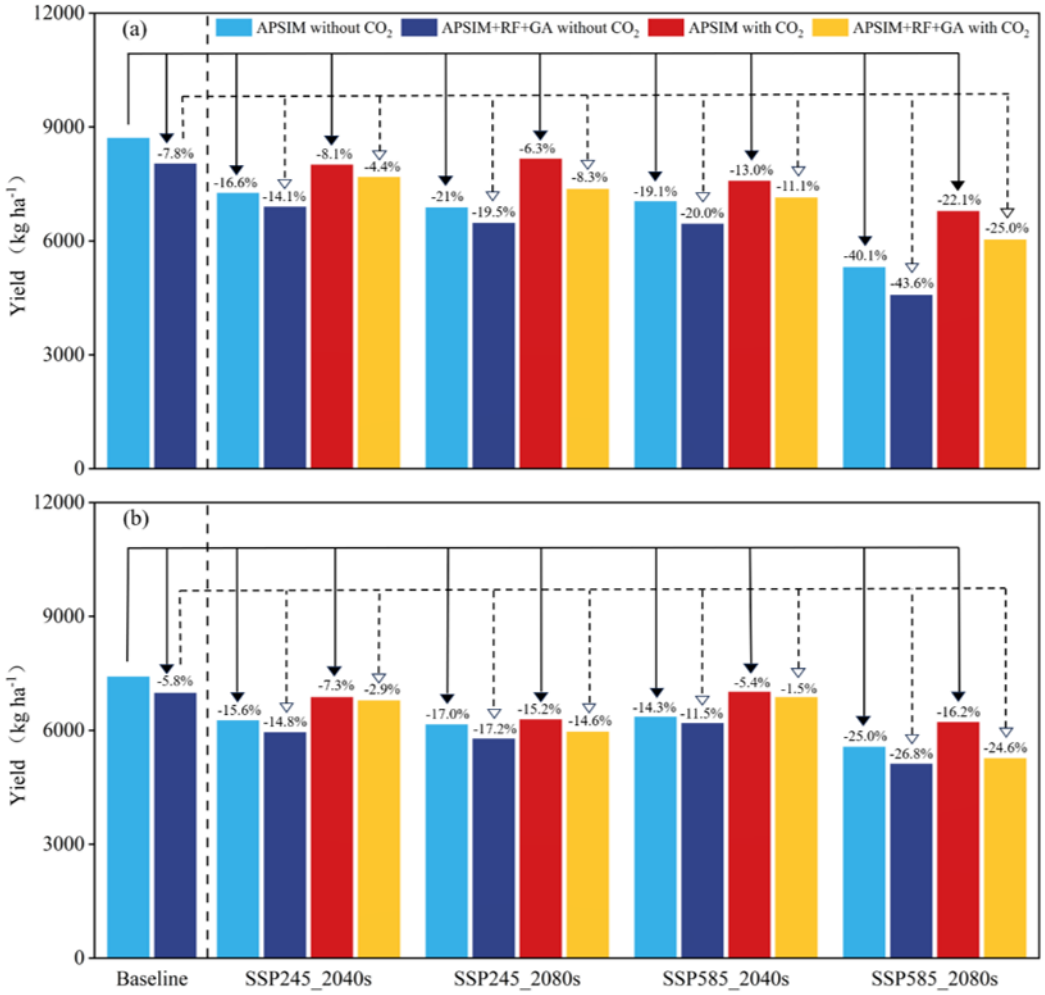


Fig. 5 Projected yield changes by GA for spring (a) and summer maize (b) in the 2040s and 2080s under SSP245 and SSP585 scenarios compared to the baseline period.

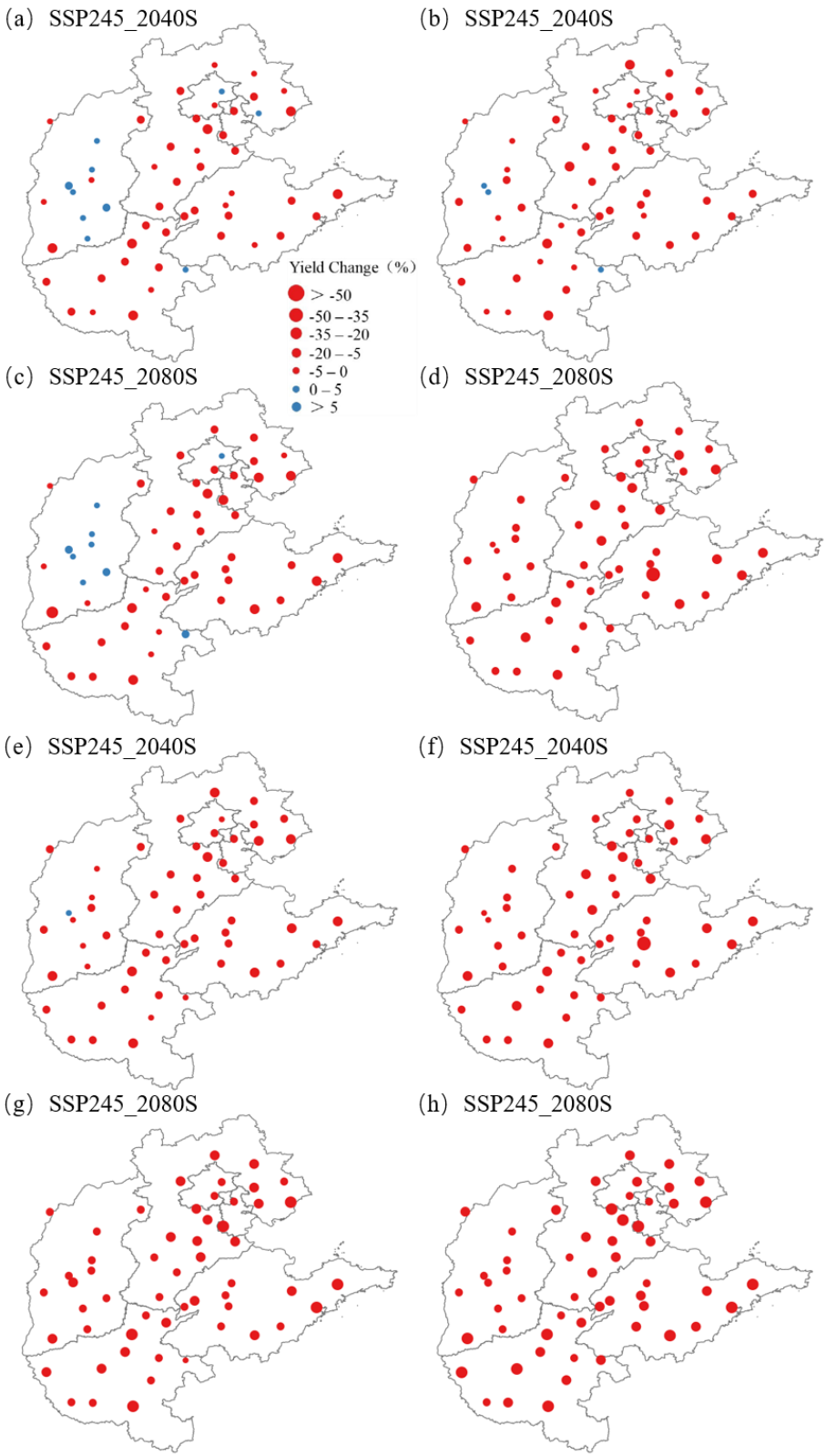


Fig. 6 Projected changes in simulated maize yield under future climate scenarios from APSIM model (a,c,e,g) and APSIM+RF+GA model (b,d,f,h) for 51 stations across the North China Plain.

Supplementary Files

This is a list of supplementary files associated with this preprint. Click to download.

- Supplementarymaterial.docx